



Detailed Investigation of Plasticized PMMA Dielectric for Improved Performance of Organic Field-Effect Transistors

Şaban Findik^{1,2} · Sadullah Öztürk³ · Osman Örnek⁴ · Raşit Köker¹ · Arif Kösemen³

Received: 18 October 2023 / Accepted: 29 January 2024 / Published online: 12 March 2024
© The Minerals, Metals & Materials Society 2024

Abstract

In this study, organic field-effect transistors (OFETs) were fabricated using plasticized poly(methyl methacrylate) (PMMA) as the gate dielectric and copper phthalocyanine (CuPc) as the active layer. Propylene carbonate (PC) was used as a plasticizer material. The dielectric properties of the plasticized PMMA were investigated in detail and the OFET parameters were examined. The effective capacitance (C_i) of plasticized PMMA was measured as $\sim 500 \text{ nF cm}^{-2}$ (at 100 Hz), which is almost 70 times higher than that of pure PMMA. This increase in effective capacitance led to significant improvements in various key parameters of the fabricated OFETs. High hole field-effect mobility values ($0.81 \text{ cm}^2 \text{ V}^{-1} \text{ s}^{-1}$), low threshold voltages ($\sim \pm 0.1 \text{ V}$), and low operating voltages (0 to $\pm 0.8 \text{ V}$) were achieved by using the plasticized PMMA dielectric. The temperature dependence of the fabricated OFETs was also investigated, and the activation energy of CuPc was estimated as 29.3 meV. The plasticized OFETs demonstrated excellent stability over 3600 measurement cycles carried out in an ambient atmosphere. This demonstrated stability of the fabricated OFETs reinforces the practical feasibility of this material combination strategy, positioning it as a key advancement in the field of solution-processable gate dielectrics.

Keywords Plasticized PMMA · organic dielectrics · low-voltage OFETs · propylene carbonate

Introduction

The primary objective of current studies is to develop functional materials that are compatible with conductors, semiconductors, and insulators. These investigations aim to facilitate the cost-effective fabrication of high-performance electronic circuits on large or flexible substrates. Organic field-effect transistors (OFETs) have been widely investigated and have attracted much attention. However, their performance at low operating voltages, high charge carrier mobility, and good device stability is not yet suitable for commercial electronics and applications.^{1–8} Further

improvements in OFET performance require global device optimization in terms of device geometry, electrical properties of the organic semiconductor, dielectric properties of the gate insulator, and control of the multiple material interfaces in the device architecture.⁹ The development of a readily applicable gate dielectric material with a high capacitance value is of great importance for the fabrication of highly stable OFETs with low operating voltage and high field-effect mobility. The capacitive property of the dielectric layer is a key parameter for lowering operating voltage of OFETs. There has been a great interest in increasing the effective capacitance (C_i) of the gate dielectric, which can be formulated by a parallel plate capacitor as shown below:

$$C_i = \epsilon_0 \frac{k}{d} \quad (1)$$

where k = the dielectric constant, d = the thickness of the insulator, ϵ_0 = the permittivity of the vacuum, and C_i is the unit-area capacitance of the dielectric materials. There are two ways to increase the C_i : either by increasing the dielectric constant k or by reducing the dielectric thickness d . Reducing gate dielectric thickness causes leakage current, which leads to a reduction in the device performance.

✉ Arif Kösemen
arif.kosemen@iuc.edu.tr

¹ Department of Electrical-Electronics Engineering, Sakarya University of Applied Sciences, Sakarya, Turkey

² Department of Computer Technology, Kırşehir Ahi Evran University, Kırşehir, Turkey

³ Institute of Nanotechnology and Biotechnology, Istanbul University-Cerrahpasa, Istanbul, Turkey

⁴ Department of Metallurgy and Materials Engineering, Kırşehir Ahi Evran University, Kırşehir, Turkey

Furthermore, reducing the gate dielectric thickness is a very delicate and costly process. The other way is to increase the dielectric constant k of the gate dielectrics. Nevertheless, the low k of organic materials is an inherent property. Various strategies have been proposed to overcome these limitations. These approaches encompass a range of methodologies, including the addition of high k dielectric nanoparticles to polymer dielectrics, the use of high k inorganic dielectrics, the creation of inorganic-organic bilayer dielectrics, and the application of self-assembly monolayer (SAM). Each of these techniques offers a separate way to improve the dielectric properties of the dielectric layer in organic field-effect transistors (OFETs).^{10–19} Recently, ion-gel gate dielectrics have been used in the construction of OFETs. Frisbie and co-workers reported that many studies of ion-gel gate dielectrics based on solid polymer electrolytes resulted in devices with high ON currents and low operating voltages due to the large capacitance of the electrolyte. The ion-gel dielectrics include triblock copolymers such as poly(styrene-*b*-methyl methacrylate-*b*-styrene) (PS-PMMA-PS) and ionic liquids such as (1-ethyl-3-methylimidazolium bis(trifluoromethylsulfonyl)imide) (EMIM TFSI).^{20–25} In addition, low operating voltages and high mobility values have been achieved by using liquid crystals as the gate dielectric material for OFET.²⁶

Poly(methyl methacrylate) (PMMA) is a well known polymer dielectric and is generally well suited for the realization of stable all-organic FETs. It has a low dielectric constant ($k < 3.5$) which limits its potential for high-performance electronics. Small molecule semiconductor-based OFETs incorporating PMMA dielectrics demonstrate high operating voltages and suffer from high pin-hole density.²⁷ To the best of our knowledge, the lowest operating voltage by using an ultra-thin PMMA dielectric layer is -8 V for a polymer-based OFET.²⁸ An interesting strategy which has not yet been adequately explored is the use of high dipole moment solvents to dissolve the polymer dielectric, modifying the interaction between the dielectric dipoles and thus keeping the polymer chain in a more extended conformation.^{29–32}

In this study, the dielectric properties of plasticized PMMA used as the dielectric layer have been investigated in detail. Stability tests of the proposed structure have been carried out and the variation of the transistor parameters with temperature has been revealed. An all-organic, non-ionic, plasticized gate dielectric was prepared by dissolving PMMA in a plasticizer, namely propylene carbonate (PC), as a high- k additive, to obtain plasticized PMMA. Dielectric properties of the plasticized PMMA have been characterized by metal-insulator-semiconductor (MIS) and metal-insulator-metal (MIM) device structures. The electrical properties of top-gate/bottom contact (TG/BC) transistors, in which the active semiconductor layer is deposited from a copper phthalocyanine (CuPc), have been investigated. The

well-studied hole transport material CuPc was used as the semiconductor because of its high thermal and chemical stability and its potential for low cost fabrication. CuPc has been extensively investigated for OFETs and according to the best of our knowledge typical values of charge carrier mobility and operating voltages around $\sim 10^{-3}$ cm² V⁻¹ s⁻¹ and -40 V have been reported.^{33,34} The plasticized PMMA was sandwiched between the gate contact and the organic semiconductor to construct the plasticized OFET as shown in Fig. 1. The operation of a plasticized OFET is quite similar to that of a conventional OFET. The temperature dependence of the devices was measured in cryogenic conditions from 50 K to 350 K. In order to test the long-term stability characteristics, bias stress measurements were performed. The investigated CuPc plasticized OFETs, which are structured organic electronic devices, exhibited low threshold (0.1 V) and operational (0.8 V) voltages, remarkably high hole mobility ($\mu = 0.81$ cm²/V s) for the CuPc active layer, and excellent stability in cyclic bias stress tests.

Experimental Section

The materials [copper(II) phthalocyanine (CuPc), poly(methyl methacrylate) (PMMA) with a molecular weight (M_w) of 120,000 g/mol, acetonitrile (ACN), and propylene carbonate (PC)] utilized in this study were purchased from Sigma-Aldrich and used as received without any purification. PMMA was dissolved in ethyl acetate as a solvent to prepare a pure PMMA solution. To enable the coating of pure PMMA onto the active layer (CuPc) using the spin coating technique at 2000 rpm, a solution with a concentration of 60 mg/ml was prepared and subsequently annealed at 110°C after the coating process. The aluminum (Al) gate electrode was deposited at a thickness of 40 nm onto PMMA using thermal evaporation.

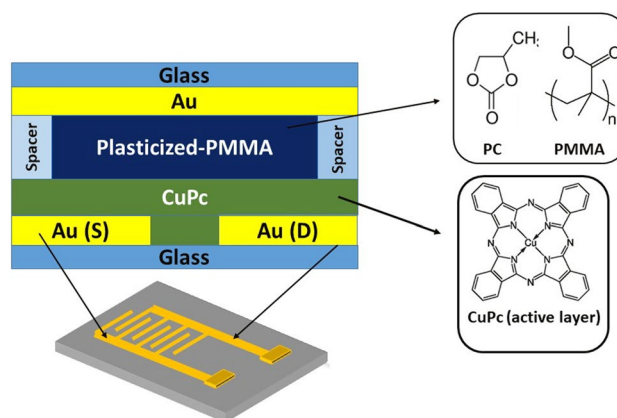


Fig. 1 Schematic of the structure of the plasticized OFET device.

The production of plasticized PMMA was executed by dissolving PMMA in ACN and subsequently incorporating propylene carbonate (PC) at a molar ratio of 70(ACN):20(PC):10(PMMA). Stirring the solution for 2 h at 200°C on a hot plate under ambient conditions yielded homogeneous plasticized PMMA in a colorless gel form. Remarkably, this gel exhibited robust stability over extended storage periods, exceeding 1 year, within a sealed container.

To examine the capacitive properties of the plasticized polymer dielectric, both metal-insulator-metal (MIM) and metal-insulator-semiconductor (MIS) structures were investigated. For the MIM structure, a plasticized polymer dielectric layer with a thickness of 50 μm was inserted between Au-coated glass electrodes. In contrast, the MIS structure consisted of a plasticized polymer dielectric layer placed between CuPc (100 nm) layer on Au electrode and an Au contact on the glass substrate. CuPc layer was deposited on the Au electrode with thermal evaporation technics. The effective area of the devices was approximately 0.25 cm^2 . These fabricated devices were characterized under ambient conditions.

The dielectric properties of the MIM and MIS structures were assessed using an HP 4194A dielectric analyzer. This suite of experimental procedures was meticulously executed to elucidate the electrical characteristics and performance of the plasticized PMMA-based dielectric material within the context of various device architectures.

The configuration of the plasticized organic field-effect transistor (plasticized OFET) is illustrated in Fig. 1. The glass substrates were cleaned with a procedure involving sequential ultrasonic baths with acetone, isopropanol, and deionized water, each for a duration of 10 min. Subsequent drying was performed under a nitrogen flow. Employing conventional photolithography techniques, interdigitated source and drain electrodes were fashioned from Cr/Au layers, with thicknesses of 5 nm and 100 nm, respectively. The

channel dimensions were established at a length of 100 μm and a width of 60 μm .

The deposition of the semiconductor layer, CuPc, was executed via thermal evaporation conducted under a high vacuum condition of 4×10^{-6} mbar, using a shadow mask to control film placement (70 nm thickness). Teflon spacers were used to fix the thickness of the plasticized PMMA dielectric layer ($\sim 50 \mu\text{m}$) by placing them on both sides of the CuPc layer. The plasticized PMMA gel was then spread uniformly over the semiconductor (CuPc) utilizing a spatula. To conclude the device fabrication process, the devices were capped with Au-coated glass, serving as the gate contact.

The electrical properties of the plasticized OFETs were investigated using a Keithley 4200-SCS, with measurements performed under ambient conditions. The stability of bias stress was explored over an extensive period, spanning 3600 cycles, which equates to more than 5 h, under ambient conditions. To analyze the temperature-dependent electrical characteristics of the OFETs, a cryogenic system was employed, encompassing a temperature range from 50 K to 350 K in a dark environment.

Results and Discussion

The electrical properties of plasticized PMMA used as a dielectric material for OFETs were thoroughly investigated in this study. The capacitive properties of this dielectric material were systematically evaluated via capacitance–voltage (C – V) measurements, using both MIS and MIM device structures (Figures S1 and S2), and by frequency-dependent capacity measurement at frequencies of 100– 10^7 Hz. As evident in Fig. 2a, extracted from Figures S1 and S2, the MIS structure exhibited distinct behaviors at 100 Hz. In particular, there was an increase in the specific capacitance when the voltage changed from positive to negative. This

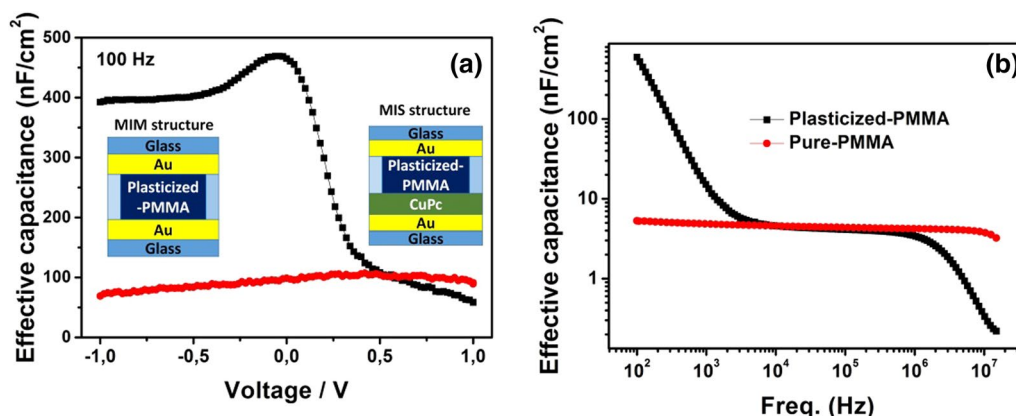


Fig. 2 (a) C – V characteristics of MIS (black) and MIM (red) structures based on plasticized PMMA dielectric. (b) Frequency dependence of the capacitance of MIS structures for PMMA and plasticized PMMA dielectrics (Color figure online).

may be attributed to the favorable accumulation of holes at the dielectric-metal interface at negative gate bias.^{35,36} The achieved capacitance peaked at an impressive value of 470 nF/cm² at 100 Hz, far exceeding the corresponding capacitance of a pure PMMA dielectric layer (~7 nF/cm² at 100 Hz for a thickness of 800 nm). Figure 2b presents the frequency (f) dependence of the capacitance characteristics of plasticized PMMA and pure PMMA in MIS structures. Frequency (f) dependence of the capacitances was evaluated between 100 and 10⁷ Hz. It is clearly seen from Fig. 2b that the capacitance of the plasticized PMMA dielectric decreases sharply in the accumulation, depletion, and inversion regions when high frequency is used. However, the capacitance of pure PMMA dielectric remains almost constant in the same region. From this observation, it can be inferred that the frequency dependency of the capacitance is a result of the presence of PC in PMMA. It is well known that the total polarization is the combination of electronic, atomic, ionic, or orientation responses of materials to an external electric field. Therefore, the improvement of the dielectric properties of plasticized PMMA by using PC may be related to several factors: (i) PC has a high k value, which increases the total dielectric constant of the layer. (ii) The high dipole moment and polarizability of PC molecules placed into PMMA polymer chains allows them to move easily in the matrix form of plasticized PMMA dielectric, which facilitates molecular motion against the electric field. (iii) The mean square end-to-end distance may increase with an increase in the dipole moment of the solvent, which is mainly due to enhanced intermolecular attraction between the polymer and PC plasticizer solvent cluster. This explanation was originally proposed by Tung et al.³⁷ for PMMA polymer chains. In that work, the polymer chains remain in more extended conformations, which may further improve the orientation of the methyl ester functional groups^{30,38,39} and their contribution to the total capacitance. C^{-2} versus V graphs were plotted for Mott–Schottky analysis for C – V measurement at 100 Hz (Figure S3). The charge density (N_A)

was calculated from the linear slope of C^{-2} versus V graphs as $\sim 7.71 \times 10^{17}$ cm⁻³ at $V_G = -0.8$ V in the semiconductor/insulator interface. Similar values have been reported for the PMMA–CuPC OFETs at $V_G = -60$ V.⁴⁰

Thermogravimetry (TG) and derivative thermogravimetry (DTG) curves of the PMMA gel material (plasticized PMMA) are shown in Figure S4, and the detailed decomposition properties of plasticized PMMA are listed in Table SI.

OFET devices were fabricated in top-gate (TG)/bottom-contact (BC) geometry. Output and transfer graphs of the plasticized PMMA-based device are given in Fig. 3. At low drain–source voltages (V_{ds}), the output characteristics exhibit favorable ohmic behavior, which transitions to saturation at higher V_{ds} levels, thereby indicating ideal performance. The leakage currents are $\sim 10^{-8}$ A, and short-channel behaviors are not observed (Figure S5). Using the subsequent equation, the field-effect mobility μ_{sat} values for the OFET can be obtained through an analysis of the saturation characteristics.⁴¹

$$\mu_{sat} = \frac{2L}{WC_i} \left(\frac{\partial(I_{ds, sat})^{1/2}}{\partial V_{gs}} \right)^2 \quad (2)$$

In this equation, I_{ds} is the drain current, V_{gs} is the gate voltage, and μ_{sat} is the saturation carrier mobility. The capacitance of the plasticized PMMA gate dielectric per unit area (C_i) at 100 Hz is denoted, while the channel width (W) is specified as 60 mm, and the channel length (L) as 100 μ m.

The transistor characteristics, charge carrier mobility (μ), threshold voltage (V_{th}), and on/off ratio ($I_{on/off}$) are extracted from the transfer curves of the plasticized and pure PMMA-based OFETs. The transfer and output curves are shown in Figs. 3 and S6 for plasticized and pure PMMA-based OFETs, respectively, and the OFET parameters are summarized in Table I. The transfer characteristics of the CuPc-based OFETs with Plasticized-PMMA dielectric were

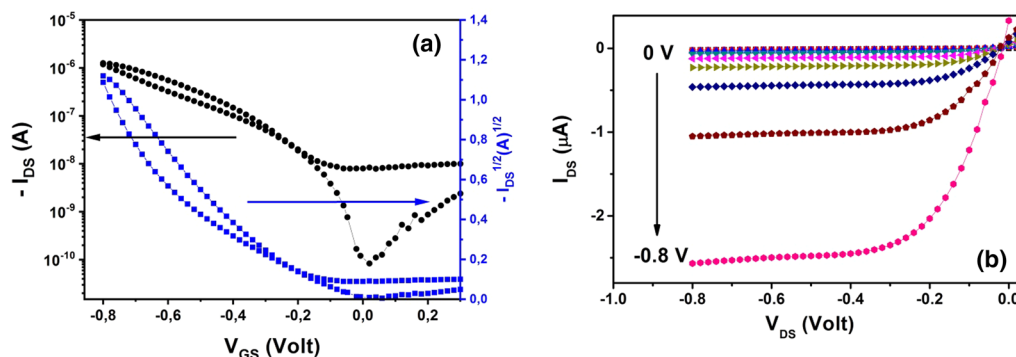


Fig. 3 (a) and (b) Transfer and output characteristics of the CuPc-based OFET on plasticized PMMA.

measured by sweeping the gate voltage (V_{gs}) from +0.3 to −0.8 V. The devices exhibit clear p -type transistor behavior at a very low operating voltage of < 1 V with a low threshold voltage (−0.1 V) and high on current (2×10^{-6} A). The average hole mobility was calculated as $0.81 \text{ cm}^2 \text{ V}^{-1} \text{ s}^{-1}$ in the saturation regime (at $V_{ds} = -0.5$ V). On the other hand, the average hole mobility for the pure PMMA device was calculated as $1.2 \times 10^{-5} \text{ cm}^2 \text{ V}^{-1} \text{ s}^{-1}$ (at $V_{ds} = 40$ V). The device demonstrates higher threshold voltages (−44 V). These results indicate that the dielectric properties of the plasticized PMMA do not only reduce the operating voltage, but also improve the OFET characteristics compared to a pure PMMA dielectric layer.

The temperature-dependent transistor characteristics of CuPc-based OFETs were investigated at temperatures ranging from 50 K to 350 K. The transfer curves are shown in Fig. 4a, and the corresponding charge carrier mobilities were calculated for each temperature (Fig. 4b). As shown in Fig. 4a, a decrease in the drain current and a negative shift in the turn-on voltage were observed as the temperature was lowered. This behavior indicates a thermally activated charge transport, which agrees well with the previous reports on pentacene- and α -sexithiophene-based OFETs.^{42–44} As shown in Fig. 4b, the mobility is found to be nearly temperature-independent in region I (50–200 K), while it increases exponentially in region II (200–350 K), which is a typical signature of thermally activated charge transport as reported by Gao et al.⁴⁵ Region II fits well to the Arrhenius equation of $\mu_{\text{eff}} \sim \exp(E_a/kT)$, where E_a is the activation energy, T is the temperature, and k is the Boltzmann constant. Based on

the slope of the linear part, the activation energy (E_a) was estimated as 29.3 meV.

A temperature-independent region with a different type of charge transport mechanism and two or more activation energies at two or more different temperature ranges was observed in early studies.^{43,46} A regular decrease in the mobility with decreasing temperature is obvious for thermally activated hopping transport.⁴⁷ In this study, we observed this kind of behavior, which can be easily seen in Fig. 4b (region I). However, in the low-temperature region (50–200 K) (region II), the mobility varies almost independently of the temperature. In this case, it can be expected that the mobility value should decrease with decreasing temperature, but the device still behaves as an average field-effect device with relatively high mobility compared to the pure PMMA-based device. The mobility of the pure PMMA-based device was measured at around $10^{-5} \text{ cm}^2/\text{V s}$ at room temperature, while the mobility of the plasticized PMMA-based device was measured at around $10^{-3} \text{ cm}^2/\text{V s}$ in the low-temperature region (50–200 K) (region II) for the CuPc active layer. This behavior can be explained by the effect of the strong polarization capability of the plasticized PMMA dielectric even at the low-temperature region. The temperature-dependent mobility observed in region I is due to the effect of shallow traps at the interfaces, and thermally activated transport can be observed because of these shallow traps. In addition, the strong polarization effect of the dielectric layer and the tunneling transport mechanism that occurs at the metal contact–organic interface in the low-temperature region may have prevented the effect of shallow

Table I Performance parameters of OFET devices

Devices	V_{th} (V)	μ ($\text{cm}^2/\text{V s}$)	$I_{on/off}$	Operation voltage (V)
CuPc pure PMMA	−44	1.2×10^{-5}	3.7×10^3	2 to (−100)
CuPc plasticized-PMMA	−0.1	8.1×10^{-1}	1.5×10^4	0.3 to (−0.8)

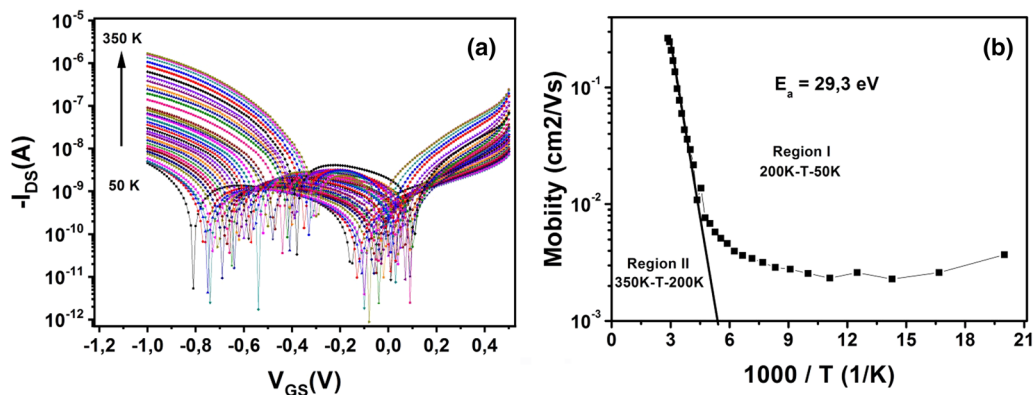


Fig. 4 (a) Transfer characteristics of CuPc and plasticized PMMA-based OFET. (b) Arrhenius plot of the saturation mobility of the plasticized PMMA-based OFET device in a temperature range of 50–350 K.

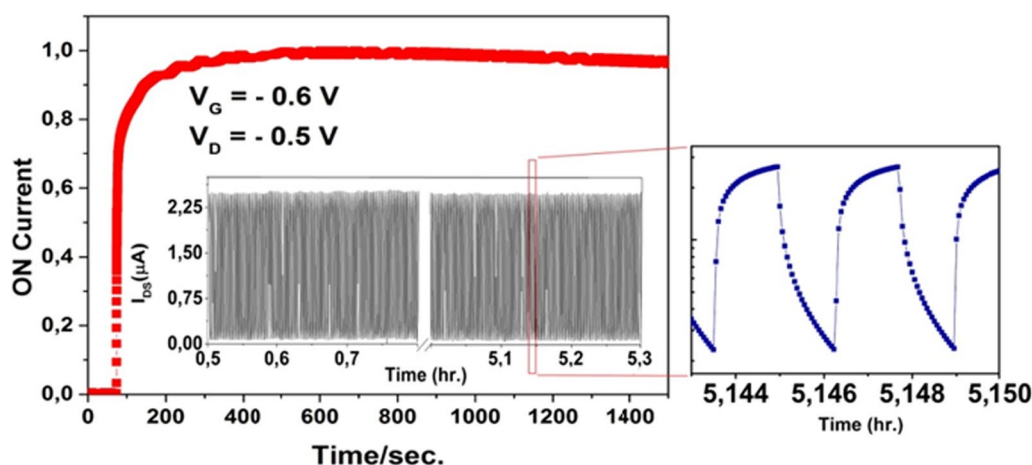


Fig. 5 Normalized ON current (I_{DS}) versus time for $V_{GS} = -0.6$ V and $V_{DS} = -0.5$ V for CuPc and PC@PMMA-based OFETs. The inset shows operational stability driven by 5-s period square-wave pulses of $V_{GS} = +0.2$ to -0.6 V and $V_{DS} = -0.5$ V.

traps and caused the formation of a temperature-independent mobility region.^{48,49}

In the next step, the device stability of the plasticized PMMA-based OFETs was investigated under bias stress conditions. Figure 5 shows the I_{ds} as a function of time under constant bias of $V_{gs} = -0.6$ V and $V_{ds} = -0.5$ V at ambient conditions. Although the bias stress was applied over 25 min, the ON current of the device remained nearly unchanged. In order to test the stability of the plasticized OFETs under dynamic stress, the gate bias (V_{gs}) was cycled repeatedly between ON and OFF states (switching frequency = 200 mHz) under ambient conditions. Plasticized PMMA-based OFETs showed negligible degradation of output characteristics after > 5 h (> 3600 cycles). These results demonstrate the impressive stability of the current of the OFETs with plasticized PMMA dielectric for technological applications.

Conclusions

In this study, we investigated a method to obtain a high-performance OFET in terms of gate dielectric material. We demonstrated that the use of a high-dipole-moment solvent of PC as a plasticizer inside PMMA dielectric is very promising material combination. The dielectric properties of the plasticized PMMA and pure PMMA were analyzed in detail. The plasticized PMMA demonstrated gate capacitance up to 470 nF/cm² at 100 Hz. Moreover, the stability of the plasticized PMMA dielectric is better than that of ion-gel or other dielectrics. The plasticized PMMA dielectric-based OFET operates at very low operating voltage, very high charge carrier mobility, and very low threshold voltage of -0.8 V, 0.81 cm²/V s, and -0.1 V, respectively, via the same charge carrier induction at low voltage relative to pure PMMA

dielectric. In the cycling bias measurement (at 200 mHz), the plasticized OFET showed almost constant ON current after more than 5 h. The μ_{sat} , threshold voltages (V_{th}), and $I_{on/off}$ were calculated in the saturation regime.

Supplementary Information The online version contains supplementary material available at <https://doi.org/10.1007/s11664-024-10974-5>.

Author Contributions All authors contributed to the study conception and design. Material preparation, data collection, and analysis were performed by ŞF, OÖ, RK, and SÖ. The manuscript was written by AK. All authors read and approved the final version of the manuscript.

Data Availability The datasets generated during and/or analyzed during the current study are available from the corresponding author on reasonable request.

Conflict of interest The authors declare that they have no known competing financial interests or personal relationships that could have appeared to influence the work reported in this paper.

References

1. K. Liu, B. Ouyang, X. Guo, Y. Guo, and Y. Liu, Advances in flexible organic field-effect transistors and their applications for flexible electronics. *npj Flex Electron.* 6, 1 (2022).
2. C. Risko and J.L. Brédas, Organic semiconductors: healing contact. *Nat. Mater.* 12, 1084–1085 (2013).
3. S. Wang, M. Kappl, I. Liebewirth, M. Müller, K. Kirchhoff, W. Pisula, and K. Müllen, Organic field-effect transistors based on highly ordered single polymer fibers. *Adv. Mater.* 24, 417–420 (2011).
4. A. Nawaz, L. Mercés, L.M. Ferro, P. Sonar, and C.C. Bufon, Impact of planar and vertical organic field-effect transistors on flexible electronics. *Adv. Matter.* 35(11), 2204804 (2023).
5. B.L. Hu, K. Zhang, C. An, W. Pisula, and M. Baumgarten, Thiadiazoloquinoline-fused naphthalenediimides for *N*-type organic field-effect transistors (OFETs). *Org. Lett.* 19(23), 6300–6303 (2017).

6. T. Lei, Y. Cao, Y. Fan, C.J. Liu, S.C. Yuan, and J. Pei, High-performance air-stable organic field-effect transistors: Isoindigo-based conjugated polymers. *J. Am. Chem. Soc.* 133(16), 6099–6101 (2011).
7. Q. Wang, E.J. Juarez-Perez, S. Jiang, L. Qiu, L.K. Ono, T. Sasaki, X. Wang, Y. Shi, Y. Zheng, and Y. Qi, Spin-coated crystalline molecular monolayers for performance enhancement in organic field-effect transistors. *J. Phys. Chem. Lett.* 9(6), 1318–1323 (2018).
8. K. Kim, J. Bae, S.H. Noh, J. Jang, S.H. Kim, and C.E. Park, Direct writing and aligning of small-molecule organic semiconductor crystals via “dragging mode” electrohydrodynamic jet printing for flexible organic field-effect transistor arrays. *J. Phys. Chem. Lett.* 8(22), 5492–5500 (2017).
9. X. Ren, Z. Lu, X. Zhang, S. Grigorian, W. Deng, and J. Jie, Low-voltage organic field-effect transistors: challenges, progress, and prospects. *ACS Mater. Lett.* 4(8), 1531–1546 (2022).
10. P. Kumar, V.N. Mishra, and R. Prakash, Ultralow-voltage eco-friendly water-induced LiOx/AlOx bilayer dielectric-based OFET. *IEEE Trans. Electron Devices* 70, 4345–4350 (2023).
11. G. Konwar, P. Saxena, V. Raghuwanshi, S. Rahi, and S.P. Tiwari, Multifunctional flexible organic transistors with a high-k/natural protein bilayer gate dielectric for circuit and sensing applications. *ACS Appl. Electron. Mater.* 4(5), 2525–2533 (2022).
12. X. Wang, H. Wang, Y. Li, Z. Shi, D. Yan, and Z. Cui, Polymer/silicon nanoparticle hybrid layer as high-k dielectrics in organic thin-film transistors. *J. Phys. Chem. C* 122(21), 11214–11221 (2018).
13. M. Halik, H. Klauk, U. Zschieschang, G. Schmid, C. Dehm, M. Schütz, S. Malsch, F. Effenberger, M. Brunnbauer, and F. Stellacci, Low-voltage organic transistors with an amorphous molecular gate dielectric. *Nature* 431(7011), 963–966 (2004).
14. M.H. Yoon, A. Facchetti, and T.J. Marks, σ - π molecular dielectric multilayers for low-voltage organic thin-film transistors. *PNAS* 102, 4678 (2005).
15. C. Kim, Z. Wang, H.-J. Choi, Y.-G. Ha, A. Facchetti, and T.J. Marks, Printable cross-linked polymer blend dielectrics. Design strategies, synthesis, microstructures, and electrical properties, with organic field-effect transistors as testbeds. *J. Am. Chem. Soc.* 130(21), 6867–6878 (2008).
16. Y. Xia, W. Zhang, M. Ha, J.H. Cho, M.J. Renn, C.H. Kim, and C.D. Frisbie, Printed Sub-2 V gel-electrolyte-gated polymer transistors and circuits. *Adv. Funct. Mater.* 20(4), 587–594 (2010).
17. L. Herlogsson, Y.Y. Noh, N. Zhao, X. Crispin, H. Sirringhaus, and M. Berggren, Downscaling of organic field-effect transistors with a polyelectrolyte gate insulator. *Adv. Mater.* 20(24), 4708–4713 (2008).
18. L. Zhang, H. Wang, Y. Zhao, Y. Guo, W. Hu, G. Yu, and Y. Liu, Substrate-free ultra-flexible organic field-effect transistors and five-stage ring oscillators. *Adv. Mater.* 25(38), 5455–5460 (2013).
19. B. Gburek and V. Wagner, Influence of the semiconductor thickness on the charge carrier mobility in P3HT Organic field-effect transistors in top-gate architecture on flexible substrates. *Org. Electron.* 11(5), 814–819 (2010).
20. W.L. Leong, N. Mathews, B. Tan, S. Vaidyanathan, F. Dötz, and S. Mhaisalkar, Solution processed non-volatile top-gate polymer field-effect transistors. *J. Mater. Chem.* 21(25), 8971 (2011).
21. J.H. Choi, Y. Gu, K. Hong, W. Xie, C.D. Frisbie, and T.P. Lodge, High capacitance, photo-patternable ion gel gate insulators compatible with vapor deposition of metal gate electrodes. *ACS Appl. Mater. Interfaces* 6(21), 19275–19281 (2014).
22. J.H. Cho, J. Lee, Y. Xia, B. Kim, Y. He, M.J. Renn, T.P. Lodge, and C.D. Frisbie, Printable ion-gel gate dielectrics for low-voltage polymer thin-film transistors on plastic. *Nat. Mater.* 7(11), 900–906 (2008).
23. K.H. Lee, S. Zhang, T.P. Lodge, and C.D. Frisbie, Electrical impedance of spin-coatable ion gel films. *J. Phys. Chem. B* 115(13), 3315–3321 (2011).
24. M.J. Panzer and C.D. Frisbie, High charge carrier densities and conductance maxima in single-crystal organic field-effect transistors with a polymer electrolyte gate dielectric. *Appl. Phys. Lett.* 20, 88 (2006).
25. H. Shimotani, H. Asanuma, J. Takeya, and Y. Iwasa, Electrolyte-gated charge accumulation in organic single crystals. *Appl. Phys. Lett.* 20, 89 (2006).
26. J. Seo, S. Nam, J. Jeong, C. Lee, H. Kim, and Y. Kim, Liquid crystal-gated-organic field-effect transistors with in-plane drain-source–gate electrode structure. *ACS Appl. Mater. Interfaces* 7(1), 504–510 (2015).
27. Y. Wang, X. Huang, T. Li, L. Li, X. Guo, and P. Jiang, Polymer-based gate dielectrics for organic field-effect transistors. *Chem. Mater.* 31(7), 2212–2240 (2019).
28. Y.Y. Noh and H. Sirringhaus, Ultra-thin polymer gate dielectrics for top-gate polymer field-effect transistors. *Org. Electron.* 10(1), 174–180 (2009).
29. N.B. Ukhah, S.P. Senanayak, D. Adil, G. Knotts, J. Granstrom, K.S. Narayan, and S. Guha, Enhanced mobility and environmental stability in all organic field-effect transistors: the role of high dipole moment solvent. *J. Polym. Sci. Part B Polym. Phys.* 51(21), 1533–1542 (2013).
30. M.A.K.L. Dissanayake, R. Jayathissa, V.A. Seneviratne, C.A. Thotawatthage, G.K.R. Senadeera, and B.E. Mellander, Polymethylmethacrylate (PMMA) based quasi-solid electrolyte with binary iodide salt for efficiency enhancement in TiO₂ based dye sensitized solar cells. *Solid State Ionics* 265, 85–91 (2014).
31. Z.A. Kösemen, A. Kösemen, S. Öztürk, B. Canımurbey, and Y. Yerli, High mobility and low operation voltage organic field effect transistors by using polymer-gel dielectric and molecular doping. *Mater. Sci. Semicond. Process.* 66, 207–211 (2017).
32. A. Kösemen, High-performance organic field-effect transistors fabricated with high-k composite polymer gel dielectrics. *J. Electron. Mater.* 48, 7819–7826 (2019).
33. I.G. Korodi, D. Lehmann, M. Hietschold, and D.R.T. Zahn, Improving the mobility of CuPc OFETs by varying the preparation conditions. *Appl. Phys. A* 111(3), 767–773 (2013).
34. L. Qin, W. Liu, J. Su, Z. Yang, Z. Liang, X. Li, P. Luan, D.-K. Wang, Z.-H. Lu, and Q. Zhu, Influence of volatile organic compound adsorption on the characteristics of organic field-effect transistors and rules for gas-sensing measurements. *Langmuir* 39(44), 15756–15765 (2023).
35. S.M. Sze, *Physics of Semiconductor Devices*, 2nd ed., (New York: Wiley, 1981).
36. Y.N. Novikov, A.A. Gismatulin, B. Hallac, Y. Roizin, and V.A. Gritsenko, Bipolar charge transport and contact phenomena in Al₂O₃. *Thin Solid Films* 781, 140004 (2023).
37. K.-L. Tung, K.-T. Lu, R.-C. Ruaan, and J.-Y. Lai, Molecular dynamics study of the effect of solvent types on the dynamic properties of polymer chains in solution. *Desalination* 192, 1–3 (2006).
38. G. Knotts, A. Bhaumik, K. Ghosh, and S. Guha, Enhanced performance of ferroelectric-based all organic capacitors and transistors through choice of solvent. *Appl. Phys. Lett.* 104, 233301 (2014).
39. N.B. Ukhah, J. Granstrom, R.R. Gari Sanganna, G.M. King, and S. Guha, Low-operating voltage and stable organic field-effect transistors with poly (methyl methacrylate) gate dielectric solution deposited from a high dipole moment solvent. *Appl. Phys. Lett.* 99, 243302 (2011).
40. M. Kraus, *Charge Carrier Transport in Organic Field-Effect Devices Based on Copper-Phthalocyanine*, University of Augsburg, (2011).

41. M.J. Panzer and C.D. Frisbie, High carrier density and metallic conductivity in poly(3-hexylthiophene) achieved by electrostatic charge injection. *Adv. Funct. Mater.* 16(8), 1051–1056 (2006).
42. T. Minari, T. Nemoto, and S. Isoda, Temperature and electric-field dependence of the mobility of a single-grain pentacene field-effect transistor. *J. Appl. Phys.* 99(3), 034506 (2006).
43. M. Abbas, A. Pivrikas, E. Arici, N. Tekin, M. Ullah, H. Sitter, and N.S. Sariciftci, Temperature dependent charge transport in organic field-effect transistors with the variation of both carrier concentration and electric field. *J. Phys. D Appl. Phys.* 46, 455105 (2013).
44. M. Schwarze, C. Gaul, R. Scholz, F. Bussolotti, A. Hofacker, K.S. Schellhammer, B. Nell, B.D. Naab, Z. Bao, D. Spoltore, K. Vandewal, J. Widmer, S. Kera, N. Ueno, F. Ortman, and K. Leo, Molecular parameters responsible for thermally activated transport in doped organic semiconductors. *Nat. Mater.* 18(3), 242–248 (2019).
45. J. Gao, K. Asadi, J.B. Xu, and J. An, Controlling of the surface energy of the gate dielectric in organic field-effect transistors by polymer blend. *Appl. Phys. Lett.* 94(9), 093302 (2009).
46. S. Mallik, S. P. Verma, S. Saha, R. Nayak, P. K. Guha, D. K. Goswami, in *IEEE International Conference on Emerging Electronics (ICEE) Conference Proceedings* 1–5 (2022)
47. H.F. Haneef, A.M. Zeidell, and O.D. Jurchescu, Charge carrier traps in organic semiconductors: a review on the underlying physics and impact on electronic devices. *J. Mater. Chem. C* 8(3), 759–787 (2020).
48. T. Minari, T. Nemoto, S. Isoda, Temperature and electric-field dependence of the mobility of a single-grain pentacene field-effect transistor. *J. Appl. Phys.* 99(3) (2006).
49. S.F. Nelson, Y.Y. Lin, D.J. Gundlach, and T.N. Jackson, Temperature-independent transport in high-mobility pentacene transistors. *J. Appl. Phys.* 72(15), 1854–1856 (1998).

Publisher's Note Springer Nature remains neutral with regard to jurisdictional claims in published maps and institutional affiliations.

Springer Nature or its licensor (e.g. a society or other partner) holds exclusive rights to this article under a publishing agreement with the author(s) or other rightsholder(s); author self-archiving of the accepted manuscript version of this article is solely governed by the terms of such publishing agreement and applicable law.